Journal of Marine Science and Technology

Volume 25 | Issue 2 Article 21

APPLICATION OF COUPLED FEM/BEM ON THE ANALYSIS OF UNDERWATER RADIATED NOISE OF A SURFACE SHIP INDUCED BY HULL VIBRATIONS

Hua-Tung Wu
Department of Engineering Science and Ocean Engineering, National Taiwan University, Taipei, Taiwan, R.O.C. Ship and Ocean Industries R&D Center, New Taipei City, Taiwan, R.O.C., wuht@mail.soic.org.tw

Pei-Tai Chen
Department of Systems Engineering and Naval Architecture, National Taiwan Ocean University, Keelung, Taiwan, R.O.C.

Journal of Marine Science and Technology, Vol. 25, No. 2, pp. 196-204 (2017)
DOI: 10.6119/JMST-016-1118-2

APPLICATION OF COUPLED FEM/BEM ON THE ANALYSIS OF UNDERWATER RADIATED NOISE OF A SURFACE SHIP INDUCED BY HULL VIBRATIONS

Hua-Tung Wu[1, 2] and Pei-Tai Chen[3]

Key words: underwater noise, finite element method, boundary element method.

ABSTRACT

This paper presents a coupled FEM/BEM for solving fluid/structure interactions under mono-frequency external loadings. The elastic structure is modeled by finite element method, and the acoustic loading is represented by boundary element method. Firstly, a semi-submerged thin shell sphere is selected as a numerical example. The numerical results are compared with the analytical solutions to verify the present method. And then, an existing vessel is selected to compute the responses of wetted surface acoustic pressures and normal velocities and, consequently, radiated underwater noise caused by the vibrating of hull structure. The results are also compared with measured data under the ship sea-trial and good correlations are obtained.

I. INTRODUCTION

The estimation of the underwater radiation energy and pattern by ships is a very important subject for some of the special purpose vessels, such as ocean research vessels and naval vessels. The underwater radiation noise induced by ship vibration may deeply affect not only the results of onboard measurement for ocean research vessel but also the characteristics of stealth for naval vessels.

The operations of a ship sailing on sea cause underwater noise due to mechanical vibrations, noise induced by propeller cavitation, and hydrodynamic noise, etc. The mechanical vibration inducing underwater noise, referring to the area of structural acoustics, is generated by ship's vibration surface contacting with sea water. As reported by Urick (1983), the vibrating of machinery generating underwater noise as ships sailing in lower speeds, that is, low frequency vibration sources, is an issue having been perusing for decades. The low frequency vibration deforms structures extending over the whole ship structures, making it difficult to control radiated underwater acoustics, while for high frequency vibrations, in general it is relatively easy to control vibration propagations through structures using convenient vibrating isolating technology, as a result, to control radiated underwater noise. Therefore, it is worthwhile to develop a numerical tool to predict such structural acoustic phenomena for ship operating in the low and medium vibrating frequencies.

Among the main excitation sources, the diesel engine is obviously one of the significant sources, especially in lower cruising speeds. For a diesel engine mounted on a ship, there are a variety of ways in which the sound is transmitted to the underwater and accommodation areas. As described by Zheng et al. (2001), the diesel engine is mounted on the supporting structures of ship hull through a large number of mechanical components. The vibration due to the diesel engine is transmitted through the supporting components into ship hull structure, thus radiating acoustic noise into water.

The coupled finite element method/boundary element method (FEM/BEM) is a conventional means of computing responses for an arbitrarily elastic structure submerged in a fluid subjected to alternating external forces. The FEM is used to describe the dynamic behavior of the structure, while the BEM is used to represent the surface acoustic loading on the structure. The coupling boundary conditions between the fluid and structure are the continuity of wetted surface normal velocity and the surface pressure acting as a loading on the structure. The standard approach to solve the structural equation in coupling with the acoustic equation is to eliminate the structural displacement variables from the two equations. By doing so, Jeans and Mathews (1990) used a variational formulation to the normal derivative of a surface boundary integral equation to deal with thin shells submerged in a fluid. The equation governing the response is a

Paper submitted 05/09/16; revised 10/06/16; accepted 11/18/16. Author for correspondence: Hua-Tung Wu (e-mail: wuht@mail.soic.org.tw).
[1] *Department of Engineering Science and Ocean Engineering, National Taiwan University, Taipei, Taiwan, R.O.C.*
[2] *Ship and Ocean Industries R&D Center, New Taipei City, Taiwan, R.O.C.*
[3] *Department of Systems Engineering and Naval Architecture, National Taiwan Ocean University, Keelung, Taiwan, R.O.C.*

symmetrically complex matrix using the pressure as a variable. Everstine and Henderson (1990) coupled the surface pressure loading, represented by a Helmholtz integral equation, with a NASTRAN program which modeled elastic structures. That investigation also implemented an out-of-core solver to resolve large-scale problems. Everstine (1991) also applied coupled FEM/BEM to deal with low-frequency resonances by treating added mass derived from the boundary integral equation at low-frequency limits. Previously numerical methods had drawbacks of dealing with problems of large degrees of freedom. Chen and Ginsberg (1995) demonstrated that the acoustic loading on the wetted surface is a complex symmetric matrix by a surface acoustic reciprocal principle. The symmetry of the acoustic loading serves as the basis for this work to formulate an efficient coupled BEM/FEM and is able to handle moderate large degrees of freedom.

In this paper, the coupled FEM/BEM is used to analyze structural vibration and underwater radiation noise of an entire ship which is excited by propulsion diesel engine. The computational results are also compared with measurements of underwater radiation noise.

II. COUPLED EQUATION FOR ACOUSTIC STRUCTURAL INTERACTIONS

In general, the structural vibration can be described by a finite element formulation. The coupling boundary condition for the coupled structural equation and acoustic equation is the continuity of the normal velocities on the wetted surface of these two equations.

The total mass matrix [M] and stiffness matrix [K] are formed by summing up the elementary matrices:

$$\begin{aligned}[M] &= \sum_e [M_e] \\ [K] &= \sum_e [K_e]\end{aligned} \tag{1}$$

The total mass/stiffness matrix can then be partitioned into the surface normal degree of freedom as denoted by a subscript symbol "n" and the remaining degrees of freedom by "i", which include the surface tangent displacements, the interior nodal points not in contact with the fluid, and all the rotational displacement.

$$\begin{aligned}[M] &= \begin{bmatrix} M_{nn} & M_{ni} \\ M_{in} & M_{ii} \end{bmatrix} \\ [K] &= \begin{bmatrix} K_{nn} & K_{ni} \\ K_{in} & K_{ii} \end{bmatrix}\end{aligned} \tag{2}$$

Correspondingly, the submerged structural equation subject to the acoustic loading and external forces oscillating at a frequency ω is

$$\begin{aligned}&\left(\begin{bmatrix} K_{nn} & K_{ni} \\ K_{in} & K_{ii} \end{bmatrix} - \omega^2 \begin{bmatrix} M_{nn} & M_{ni} \\ M_{in} & M_{ii} \end{bmatrix} \right) \begin{Bmatrix} x_n \\ x_i \end{Bmatrix} \\ &= \begin{Bmatrix} f_n \\ f_i \end{Bmatrix} + \begin{Bmatrix} -N^T P \\ 0 \end{Bmatrix}\end{aligned} \tag{3}$$

where M_{pq} ($p, q = n, i$) are global mass matrices corresponding to the n and i degrees of freedom, x_n and x_i are the corresponding displacement variables, f_n and f_i are the associated external alternating forces, P is the discretized surface pressure, and N is a shape factor matrix arising from shape functions in discretizing the normal displacement and surface pressure. The shape factor matrix can be identified by considering the virtual work $\delta\bar{W}$ done by the surface pressure against the structure's virtual normal displacement δw:

$$\begin{aligned}\delta\bar{W} &= \int P \delta w dS \\ &= \int_S \left[\sum_e \left(\sum_i P_i \psi_{i,e} \right) \right] \left[\sum_e \left(\sum_j \delta x_{n,j} \phi_{j,e} \right) \right] ds \\ &= \sum_i \sum_j P_i \delta x_{n,j} \int_S \left(\sum_e \psi_{i,e} \right) \left(\sum_e \phi_{j,e} \right) ds \\ &= \sum_i \sum_j P_i \delta x_{n,j} N_{ij}\end{aligned} \tag{4}$$

where $\psi_{i,e}$ and $\phi_{j,e}$ are the shape functions for pressure and normal displacement, and the expression $\sum_e \left(\sum_i P_i \psi_{i,e} \right)$ is the interpolated pressure on the surface in terms of the nodal pressure P_i. The inner summation denotes a contribution of the interpolated pressure form an individual element, while the outer summation represents the contribution from all the elements on the surface. A similar expression can be used for the displacement. The coefficients N_{ij} are the coefficients of the shape factor matrix N.

The surface acoustics relating the surface pressure and normal derivative of the surface pressure is described by a boundary Helmholtz integral equation:

$$\left(1 - \Omega(x)\right) P(x) = \int \left[P(y) \frac{\partial G_h(x,y)}{\partial n(y)} - \frac{\partial P(y)}{\partial n(y)} G_h(x,y) \right] dS_y \tag{5}$$

where x is a field point, y is a source point, dS_y is the differential area integrating with respect to source point y, $\partial P/\partial n$ is the pressure normal derivative, and $G_h(x, y)$ is the half-space Green's function for a semi-immersed body which is detailed described by Chen et al. (2002).

The $\Omega(x)$ is defined by:

$$\Omega(x) = -\frac{1}{4\pi} \int \frac{\partial \left(1/|x-y| \right)}{\partial n(y)} dS_y \tag{6}$$

which is the solid angle at point x subtended over the wetted surface of the interior domain. Note that the oscillation time factor is $e^{i\omega t}$, where ω is oscillating frequency. The pressure normal derivative relates to the normal displacement as

$$\frac{\partial P}{\partial n} = -i\rho_0 \omega v_n = \rho_0 \omega^2 x_n \tag{7}$$

where ρ_0 is the fluid density. Discretizing P and $\partial P/\partial n$ in Eq. (5) leads to the matrix equation,

$$[H]\{P\} = [G_h]\left\{\frac{\partial P}{\partial n}\right\} \tag{8}$$

where $\{P\}$ and $\{\partial P/\partial n\}$ are discretized nodal values, and $[H]$ and $[G_h]$ are complex matrices. By combining Eqs. (7) and (8), the surface pressure $\{P\}$ relates to the normal displacement $\{x_n\}$ as

$$\{P\} = [H]^{-1}[G_h](\rho_0 \omega^2)\{x_n\} \tag{9}$$

Substituting the above equation into Eq. (3) leads to the equation for forced vibration of the submerged structure:

$$\begin{bmatrix} D_{nn} & D_{ni} \\ D_{in} & D_{ii} \end{bmatrix}\begin{Bmatrix} x_n \\ x_i \end{Bmatrix} + \begin{bmatrix} \rho_0 \omega^2 N^T [H]^{-1}[G_h] & 0 \\ 0 & 0 \end{bmatrix}\begin{Bmatrix} x_n \\ x_i \end{Bmatrix} = \begin{Bmatrix} f_n \\ f_i \end{Bmatrix} \tag{10}$$

where D_{pq} ($p, q = n, i$) are identified as

$$D_{pq} = K_{pq} - \omega^2 M_{pq} \tag{11}$$

The second term of the first equation in Eq. (10) is the acoustic loading which only applies to the normal displacement x_n. The effects of the acoustic loading on x_i is through the matrices D_{ni} and D_{in}. Eq. (9) reveals that the acoustic loading is equivalent to an additional complex stiffness matrix on the normal degree of freedom.

III. NUMERICAL VALIDATION

A numerical example with constant thickness spherical shell under concentrated external force is selected to validate the present numerical method. The spherical shell has a lower semisphere submerged in the fluid. The material data for the spherical shell are listed as follows: the radius of the shell is 1 m, the thickness of the shell is 0.03 m, Young's modulus is 2.07×10^{11} Pa (N/m^2), the Poisson ratio is 0.3, the densities of the shell and water are 7669 and 1000 kg/m^3, respectively, and the sound speed of the water is 1524 m/s. An external concentrated alternating force is exerted at the bottom apex.

Fig. 1 shows the finite element mesh of the spherical shell. There are 1698 nodal points and 1696 shell elements. An external alternating point force with constant amplitude of one Newton is applied at the bottom apex of the shell. Previous literature provides the analytical solution for the spherical shell (Chen et al., 2002, 2005).

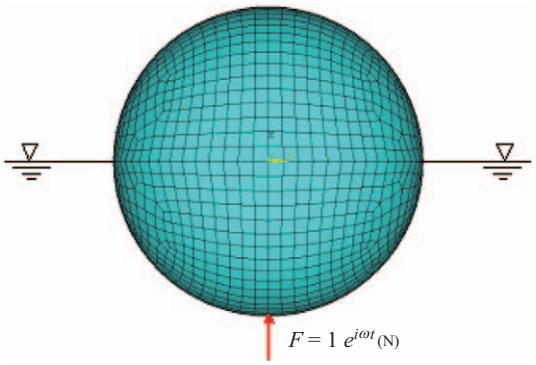

Fig. 1. FEM mesh of spherical shell.

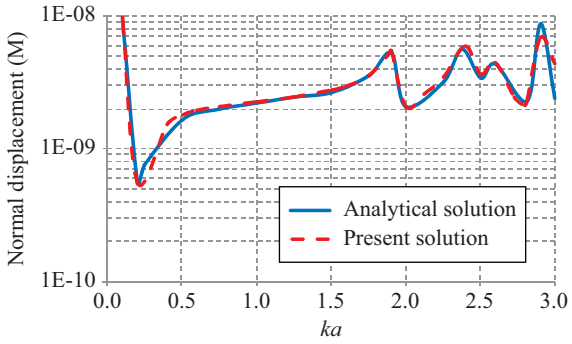

Fig. 2. Frequency dependence for the normal displacements on the bottom apex.

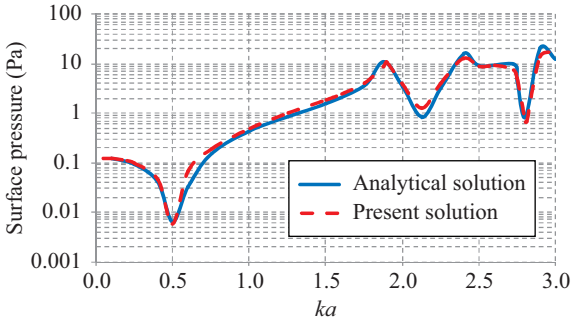

Fig. 3. Frequency dependence for the surface pressures computed on the bottom apex.

Figs. 2 and 3 show the normal displacement and surface pressure at the bottom apex versus scanning exciting frequencies. Fig. 4 shows the normal displacements along a non-dimensionalized arc length of the sphere computed by present method where the non-dimensionalized arc length is the ratio of arc distance from the top apex, s to the total arc length, s_0. Once the x_n is known, the surface pressure is computed and presented in Fig. 5. The non-dimensionalized frequencies ka are 1.6 and 2.4. Where k is a wave number defined as $k = \omega/c$,

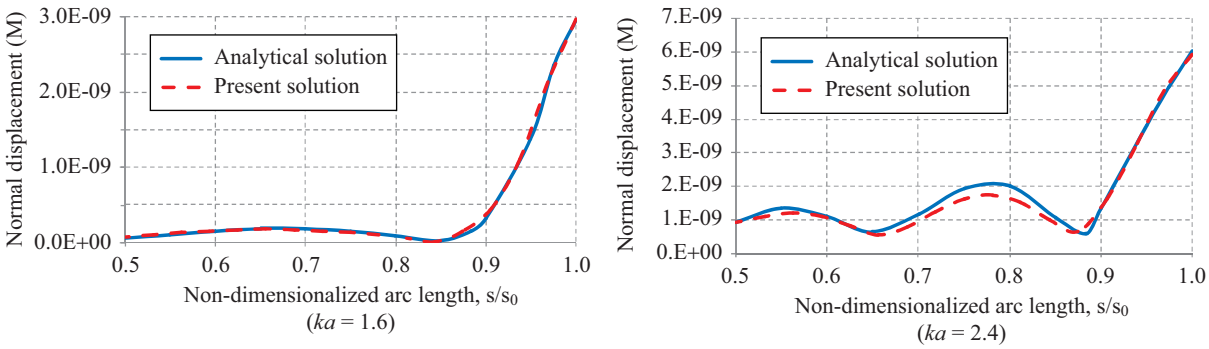

Fig. 4. Comparison of normal displacements along an arc length of the sphere vibrating at frequencies *ka* = 1.6, 2.4.

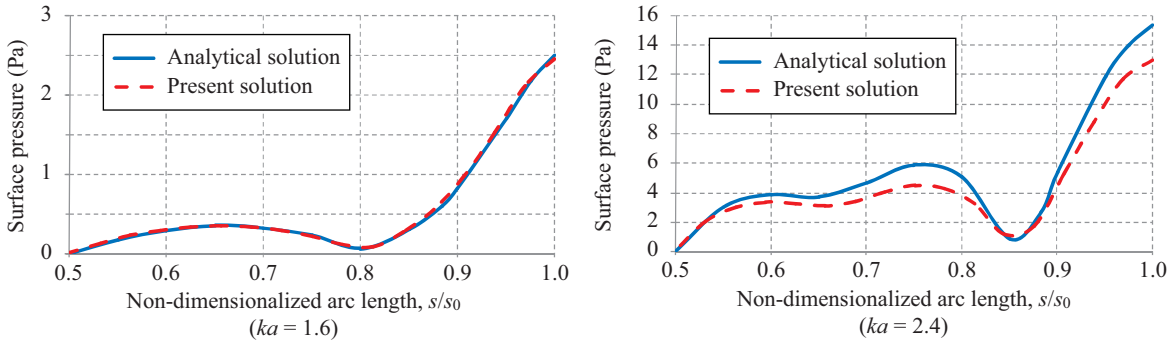

Fig. 5. Comparison of surface pressures along an arc length of the sphere vibrating at frequencies *ka* = 1.6, 2.4.

and c is the sound velocity, a is the radius of the shell.

The results of present method shown on Figs. 2-5 are also compared with those of analytical solutions. According to Figs. 2-5, good correlations are archieved at low frequencies and minor discrepancies are observed with incresing frequencies. It is expected that the errors could be reduced by further refining the meshes.

IV. MAIN ENGINE EXCITED UNDERWATER RADIATION NOISE OF AN EXISTING VESSEL

1. FEM Model

An existing 60M high speed vessel designed by SOIC (Ship and Ocean Industries R & D Center) is selected to calculate the underwater radiation noise induced by the excitation of diesel engine (Wu et al., 2005). Fig. 6 shows the FEM model of the subject high speed vessel which contains about 5400 nodal points and 13500 elements including shell, beam and rod elements. The decks, bulkheads and the hull are modeled as shell elements. Beam and rod elements are used to model the stiffeners and pillars. Large mechanical equipments such as main engines are modeled as solid elements, and other smaller components with large concentrated mass are modeled as lumped mass elements. The mass densities for each parts of the FEM model are adjusted to make sure that the mass distribution of the whole ship model is almost identical to the design condition.

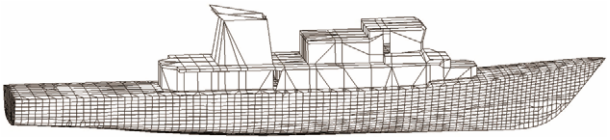

Fig. 6. FEM model of the 60M high speed vessel.

There are about 1900 nodal points and 1950 shell elements in the hull's exterior wetted surface that is in contact with water. Those exterior nodes and elements are treated as the BEM model to take the fluid acoustic loading interacting with underwater radiation noise.

2. Excitation Forces

The sources of radiation noise on ships can be grouped into three major classes, namely machinery noise, propeller noise and hydrodynamic noise. In general, the propeller will not only excite the ship hull vibration but also produce the strong underwater noise itself, that is, the underwater noise induced by propeller is more complex and we need to pay more further efforts on the related studies. Besides the propulsion propeller, the main diesel engine is the most important excitation source onboard. Thus, in this paper, only the underwater radiation noise which is induced by the main diesel engine exciting hull vibration is to be considered.

Diesel engine excitation is composed of many harmonic components dependent on the rotational velocity of the engine. The

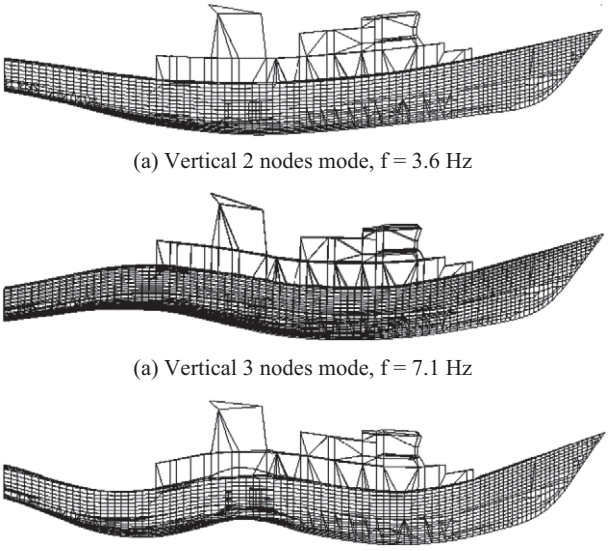

(a) Vertical 2 nodes mode, f = 3.6 Hz

(a) Vertical 3 nodes mode, f = 7.1 Hz

(a) Vertical 4 nodes mode, f = 10.7 Hz

Fig. 7. Mode shapes calculated by MSC/NASTRAN.

Table 1. Fundamental natural frequencies & peak frequencies calculated by present method (Hz).

MSC/NASTRAN		Present	
Mode	Frequency	Peak No.	Frequency
2 nodes	3.6	1	3.6
3 nodes	7.1	2	7.2
4 nodes	10.7	3	10.7

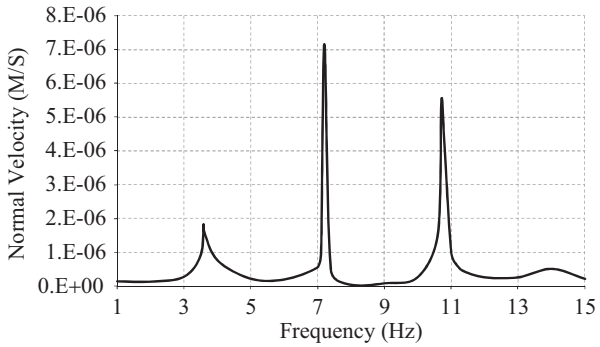

Fig. 8. Frequency response of normal velocity at stern bottom shell.

diesel engine excitations could be calculated according to the mass of pistons, strokes, firing order, …, etc. However, the most precise and effective data could be obtained from a test-bed trial given by the diesel engine manufacturer.

According to the excitation forces/moments provided by the engine manufacturer of this vessel, there is no significient 1st and 2nd order excitations, but 4th order external unbalanced moment and force could be found. Thus, only the 4th order unbalanced moment and force provided by the main engine manufacturer are considered as excitations for the numerical analysis.

3. Hull Structure Fundamental Modes

The hull structure normal mode analysis of this ship had been performed at the design stage. The FEM structural model is the same as described above and the added mass of submerging wetted surface is calculated by using the MSC/NASTRAN built-in "virtual mass method". Since the ship is freely floating on the water surface, there is not any additional displacement restrained condition specified for the normal mode analysis. The natural frequencies of the first 3 fundamental elastic vertical bending modes, e.g., 2-nodes, 3-nodes & 4-nodes modes, calculated by using MSC/NASTRAN were identified to be 3.6 Hz, 7.1 Hz and 10.7 Hz respectively. Fig. 7 shows the mode shapes of these three fundamental modes obtained from MSC/NASTRAN.

In this paper, a couple of constant unit unbalanced forces are applied at the C.G. of both main diesel engines as excitation sources, and perform a series of frequency scan calculations by using the present coupled FEM/BEM method from 1 Hz to 15 Hz, which is expected to cover the frequency range of major fundamental hull girder elastic modes of this ship.

Fig. 8 shows the normal velocity of a node located at stern bottom under various exciting frequencies. There are 3 major peaks can be found in Fig. 8 obviously. The corresponding frequencies of these three peaks are 3.6 Hz, 7.2 Hz and 10.7 Hz respectively. A comparison of natural frequencies is listed in Table 1. It can be found that the first 3 peak frequencies found in the calculation results are quite close to the results of previous normal mode analysis by using MSC/NASTRAN.

It is instructive from the aspect of practical engineering applications to make some comments of the results presented in Figs. 7 and 8. Eq. (12) describes the dynamic equation for coupled elastic and acoustics equations where the infinite extent acoustic domain is converted to a boundary integral equation (e.g., BEM). The elastic structure and acoustics domain interact each other at the surface contacting with water by imposing the continuity of the surface normal velocity of structural deformation and acoustic particle oscillation, as well as the acoustic surface pressure as the external load applying to the surface. Here the acoustic loading term in Eq. (10) is $\rho_0\omega^2 N^T[H]^{-1}[G_h]$, which can be divided as real and imaginary parts, where the real part exhibits as added mass effect, while the imaginary part refers to acoustic radiating effect propagating into far field, which is unwanted to be detected. Hence, the imaginary part plays the role for acoustic noise radiating into water, responding for acoustic stealth for underwater vehicles. The Eq. (10) can be rewritten as:

$$\left([M]+[M_a]\right)\{\ddot{x}\}+[D_a]\{\dot{x}\}+[K]\{x\}=\{f\} \qquad (12)$$

where $[M_a]$ denotes the real part of aforementioned acoustic loading matrix, while $[D_a]$ is the corresponding imaginary part, indicating radiation damping effect.

The computation using MSC/NASTRAN with built-in "virtual

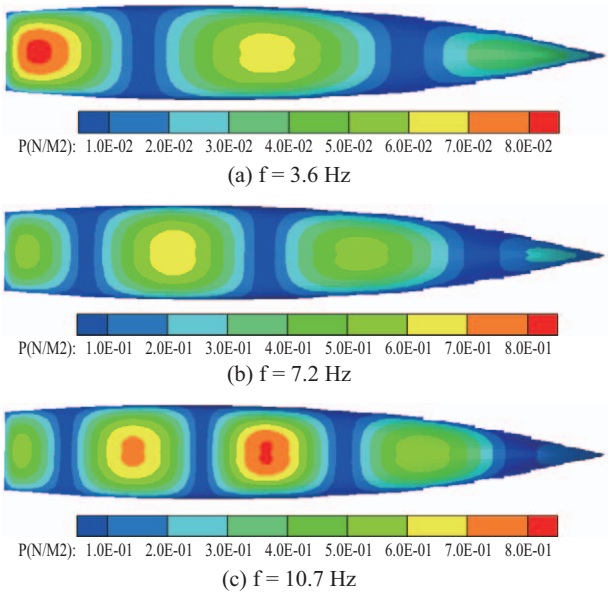

Fig. 9. Surface pressure distribution near peak frequencies calculated by using coupled FEM/BEM.

mass" is to neglect the damping matrix $[D_a]$, and consequently, to perform standard normal mode extraction, where the first three modes as shown in Fig. 7. This is a very practical and essential way for engineers to understand the dynamic characteristics of ships. However, the solved responded displacement $\{x\}$ in Eq. (12) is not able to be used to predict underwater noise, simply because the neglecting of the damping matrix $[D_a]$ in Eq. (12). This solved $\{x\}$ is in-phase or out-phase with the external force, or equivalently, the phase of responded velocity is $\pi/2$ with the external force, resulting no net power delivered out of the structure, thus no acoustic power radiating to far field. The contribution of the damping matrix is small at low frequency, while the corresponding added mass matrix $[M_a]$ is significantly large. Notably reveled by Fig. 8, the sharp peaks indicate clearly that the radiation damping is very small as compared with mass and stiffness effects.

Fig. 9 shows the surface pressure distribution near peak frequencies calculated by using the present coupled FEM/BEM. With compared to the calculated mode shapes, relatively lower surface pressures can be found near those regions of vibration "nodes" shown in Fig. 7.

4. Numerical Results of Underwater Radiation Noise

The sources of radiation noise on ships can be grouped into three major classes, namely machinery noise, propeller noise and hydrodynamic noise. In this paper, we consider only the underwater radiation noise induced by engine excitations. Only the clutch-off idle speed conditions are selected to perform the numerical analysis.

Figs. 10 and 11 show the calculated contours of normal velocity and sound pressure on wetted surface under the 4th order unbalanced moment/force excitation of port side main

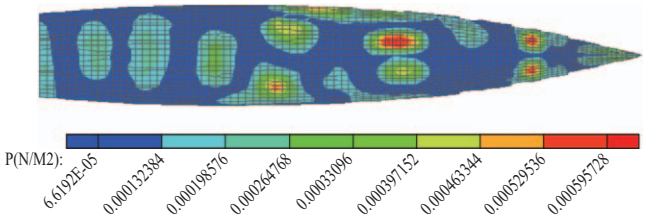

Fig. 10. Normal velocity distribution on wetted surface (port side engine excited).

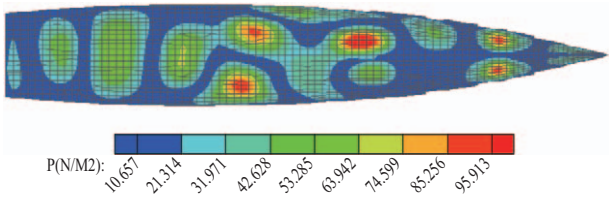

Fig. 11. Sound pressure distribution on wetted surface (port side engine excited).

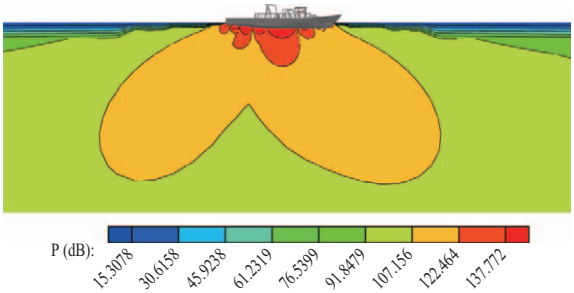

Fig. 12. Underwater radiated sound pressure distribution at C.L. plane (port side engine excited).

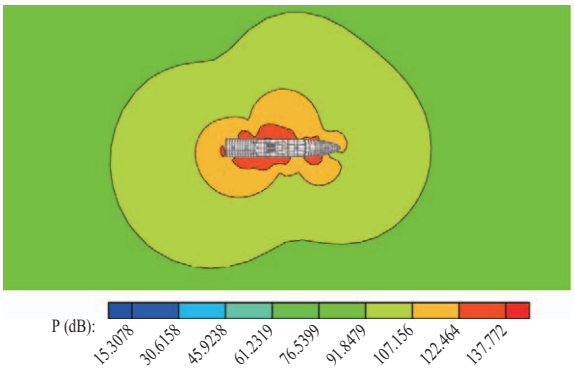

Fig. 13. Underwater radiated sound pressure distribution at a plane of 5M below water surface (port side engine excited).

engine at idle speed. Figs. 12-14 show the sound pressure distributions of underwater radiation noise at C.L. plane, horizontal plane at a distance of 5M below water surface and midship transverse section respectively under the same port side engine excitation condition. While Fig. 15 shows the sound

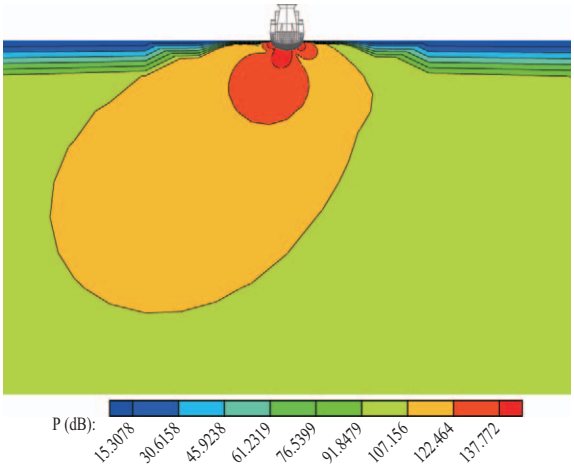

Fig. 14. Underwater radiated sound pressure distribution at midship transverse plane (port side engine excited).

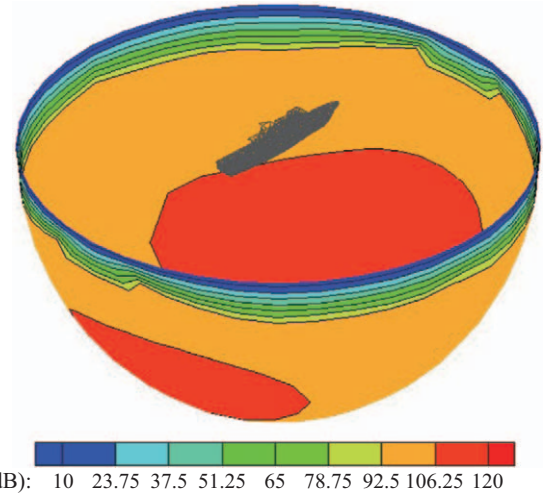

Fig. 15. Underwater radiated sound pressure distribution at a distance of 100M away from the center of midship at water surface (port side engine excited).

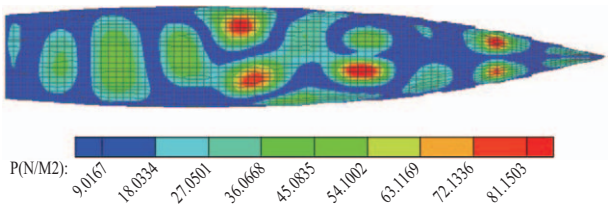

Fig. 16. Sound pressure distribution on wetted surface (stbd. side engine excited).

presssure distribution of underwater radiation noise at a semi-spherical surface with distance of 100M away from the center of midship at water surface.

Fig. 16 shows the calculated contours of sound pressure on wetted surface under the 4th order unbalanced moment/force excitation of starboard side main engine at idle speed. Fig. 17 shows the sound pressure distributions of underwater radiation noise at midship transverse section under the same starboard side engine excitation condition.

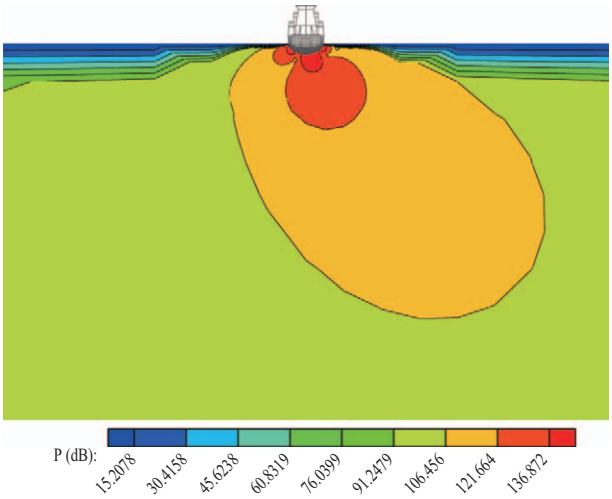

Fig. 17. Underwater radiated sound pressure distribution at midship transverse plane (stbd. side engine excited).

In general, the distributions of wetted surface normal velocity as well as the sound pressure are similar and symmetrical while the ship structure is excited by port and starboard side main engine respectively. The major reason for slightly differences between the calculation results of port and starboard side engine is mainly due to the unsymmetrical structure arrangement of the ship.

5. Comparison with Onboard Measurements

A series of underwater radiation noise measurements was performed at a selected sheltered area with depth of water more than 200M during the test sailing of the ship. Several cases of measurements were carried out, such as the underwater radiation noise measurement while the ship was still or running. The hydrodynamic pressure pulse on the stern bottom shell surface above propeller and near/far field underwater radiation noise was also measured and recorded. (Wu et al., 2004).

To exclude the effect of propeller noise and compare with the numerical calculation results. The measurement results while the ship was still and either port or starboard side engine was declutched and running in idle speed (420 RPM) were choosen for the comparison.

Two hydrophones were installed to measure the underwater sound pressures generated by the ship. An external hydrophone was lowered along the starboard hull side near the midship, the depth of hydrophone was 5M below the still water surface, as shown in Fig. 18. Another hull-mounted hydrophone was installed on the bottom shell above the starboard side propeller, as shown in Fig. 19. The hull-mounted hydrophone was also used to obtain the radiated noise signal from propulsion propellers while the ship was sailing in higher speeds.

Table 2. Comparison of sound pressure levels between numerical and measurement results.

Engine speed (RPM)	4th order freq. (Hz)	Position	Numerical (dB re. 1 × 10^{-6} Pa)	Measurement (dB re. 1 × 10^{-6} Pa)
425 (Stbd. Engine)	28.3	Midship stbd. side*	134.4	131.5
		Stern bottom shell	148.7	147.8
425 (Port Engine)		Midship stbd. side*	133.9	137.1
		Stern bottom shell	148.8	147.4

*5M below still water surface

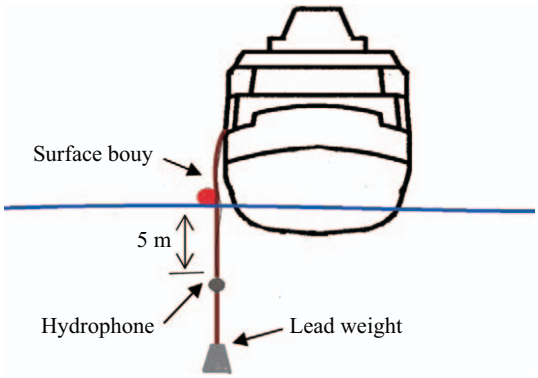

Fig. 18. Hydrophone lowered along the hull side.

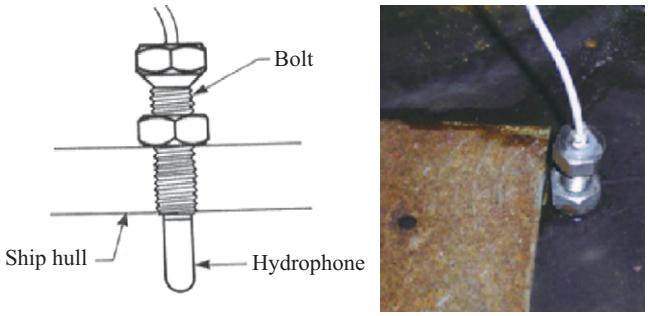

Fig. 19. Hull-mounted hydrophone.

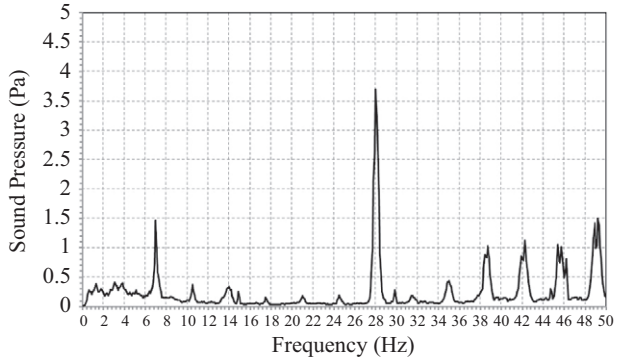

Fig. 20. Sound pressure spectrum while starboard main engine running (Midship external hydrophone).

Fig. 20 shows the spectrum of measured sound pressure of the midship external hydrophone while the starboard side main engine is running. Firstly, it is noted that a response peak can be found at around 7.1 Hz, which is very close to the 3-nodes fundamental hull girder mode as mentioned above. And it is suspected to be excited by ambient excitations of machines and waves.

Besides, a major response peak can be found near 28 Hz, which can be identified to be the 4th order of main engine speed of 420RPM. This response peak is induced by the vibration source of 4th order of engine operation. Some other minor responses can also be found in Fig. 20, which are suspected to be excited by the internal guide forces of main engine or other auxiliary machines onboard.

To compare with the numerical results, the sound pressure level excited by the 4th order main engine external unbalance force/moment near the peak of 28Hz can be obtained as:

$$SPL = 20\log\left(P_{rms}/P_0\right) \tag{13}$$

where P_{rms} is the 1Hz band width root mean squared sound pressure with center frequency at the desired peak frequency (28 Hz). $P_0 = 10^{-6}$ Pa is the reference sound pressure in water.

Table 2 shows the position and comparison between numerical calculation and measurement results. Generally, good correlations can be found between the numerical calculation and measurement results. In addition, it can be found that the measured sound pressure level of the hydrophone at midship starboard side while the starboard side main engine running is somewhat lower than that of port side main engine running. Unfortunately, it is not easy to identify the key factor which may cause the variations of measurement, since there are many unknown environment factors may affect the measurement results such as wind, wave and seabed conditions …, etc. However, the differences between the numerical and measurement results shown in this paper are not significant and can be acceptable.

V. CONCLUDING REMARKS

This paper presents a numerical method for computing the response and acoustic radiation for semi-immersed elastic structures by using the coupled BEM/FEM. Effectiveness of the numerical method is verified by an analytical solution of a spherical thin shell semi-immersed in water. A good correlation is found at low frequencies and minor discrepancies with increasing frequency.

An existing 60M high speed vessel is also selected to calculate the underwater radiation noise induced by the excitation of diesel engine in this paper. Some peak frequencies can be found in the frequency scan calculation results of normal velocity on stern bottom shell and those peak frequencies are found to be quite close to the fundamental natural frequencies found in the normal mode analysis by using MSC/NASTRAN at the design stage of this ship. The calculations of underwater radiation noise under the unbalanced moment/force excitations of main engines are also performed. Good correlations can be found between the numerical calculation and measurement results.

In general, for higher excitation frequency, finer mesh is necessary and the numerical model may get larger. And it may become much time consume and need more computing resources to perform the numerical calculation. For example, a rough comparison can be made between the two numerical models in this paper. It takes about 3 minutes for the semi-immersed spherical shell model presented in this paper for one exciting frequency, while it takes about 50 minutes for the model of 60M high speed vessel. It is found that computing time increases significantly as the nodal numbers is increased.

REFERENCES

Chen, P. T. and J. H. Ginsberg (1995). Complex power, reciprocity and radiation modes from submerged bodies. Journal of Acoustical Society of America 98, 3343-3351.

Chen, P. T., C. S. Lin and T. Yang (2002). responses of partially immersed elastic structures using a symmetric formulation for coupled boundary element and finite element methods. Journal of Acoustical Society of America 112(3), 866-875.

Everstine, G. C. and F. M. Henderson (1990). Coupled finite element/boundary element approach for fluid-structure interaction. Journal of Acoustical Society of America 87, 1983-1947.

Everstine, G. C. (1991). Prediction of low frequency vibrational frequencies of submerged structures. Journal of Vibration and Acoustics 113, 187-191.

Jeans, R. A. and I. C. Mathews (1990). Solution of fluid-structure interaction problems using a coupled finite element and variational boundary element technique. Journal of Acoustical Society of America 88, 2459-2466.

Urick, R. J. (1983). Principles of Underwater Sound, 3rd ed., McGraw-Hill Book Company, New York.

Wu, H. T, P. T. Chen, C.H. Liu and C.Y. Lu (2005). The estimation of underwater noise induced by engine vibration. Proceedings of the 19th Asian Technical Exchange and Advisory Meeting on Marine Structures, TEAM'2005 Singapore, 248-255.

Wu, H. T. (2004). Investigation on radiated underwater noise of ships, SOIC Technical Report No. USDDC-221-T822. (in Chinese)

Zheng, H., G. R. Liu, J. S. Tao and K.Y. Lam (2001). FEM/BEM analysis of diesel piston-slap induced ship hull vibration and underwater noise. Applied Acoustics 62, 341-358.